Point defects in YAG ceramics induced by SiO_2 and MgO sintering additives. A first principle study

M. Vovsianiker[1], L. Kravchenko[1], D. Fil[1,2]
[1]Institute for Single Crystals NAS of Ukraine, [2]V. N. Karazin Kharkiv National University

Introduction

Yttrium aluminum garnet (YAG) doped with rare-earth or transition-metal ions is widely used as a laser material. Besides being grown as single crystals, YAG can be produced as transparent ceramics, whose optical and mechanical characteristics are comparable to those of single crystals. Ceramic technology also offers several practical benefits: lower manufacturing costs, higher achievable doping levels, and the ability to fabricate multilayer structures with a spatially varying composition. At the same time, the optical quality of transparent ceramics depends strongly on residual porosity, secondary phases, and grain boundaries, and all of these are largely determined by the sintering process.

Sintering additives are commonly employed to obtain laser-grade ceramics. For YAG, tetraethyl orthosilicate (TEOS) and SiO_2 are the most common sintering aids. Recent experiments have shown that MgO is a promising additive that inhibits grain growth in YAG ceramics, and a number of studies have used it together with SiO_2 or TEOS. As reported in [1], YAG ceramics sintered with SiO_2 and MgO at equal atomic concentrations of Si and Mg contained numerous residual pores. These pores scattered light strongly and made the samples almost opaque. By contrast, ceramics sintered with an excess of either SiO_2 or MgO showed considerably better optical quality, with the best results obtained for the Si-enriched samples.

This work presents the results of an extensive first-principles study of Si and Mg doping in YAG. The formation energies and equilibrium concentrations of point defects in Si-doped, Mg-doped, and Si-Mg co-doped YAG were calculated as functions of the sintering conditions.

Calculation methods

Defect formation energy calculations were performed using the SIESTA software package [2]. Pseudopotentials are generated with the Optimized Norm-Conserving Vanderbilt Pseudopotential approach [3].

Formation energy of i-type defect is given by the equation[4,5]:

$$E_i = E_{def,i} - E_{perf} - \sum_x \mu_x p_{x,i} + \mu_e q_i + E_i^{(c)},$$

where $E_{def,i}$ is the total energy of a cell with i-type defect,
E_{perf} is the total energy of a cell without any defects,
μ_x and $p_{x,i}$ are the chemical potential and the number of x-type atoms that are added to ($p_{x,i} > 0$) or are removed from ($p_{x,i} < 0$) cell,
μ_e is the electron chemical potential,
q_i is the defect electrical charge (in units of |e|),
$E_i^{(c)}$ is the correction that excludes electrostatic interaction caused by periodic copying of charged defects in the calculations.

Calculation methods

Calculations were performed for the Al_2O_3-rich and $YAlO_3$-rich conditions. The formation energies of defects under these conditions differ only slightly for most defects. In the following, **we present results for crystals grown in the Al_2O_3-rich environment**. To calculate the chemical potentials of the host elements, the formation energies of Al_2O_3 and Al were calculated. Structural data of compounds were taken from OQMD [6]. The chemical potential of Mg was determined from the equilibrium condition with $MgAl_2O_4$. The chemical potential of Si was taken as the lower of the two values imposed by equilibrium with elemental Si and with Y_2SiO_5.

We considered the oxygen chemical potential varying from reducing conditions (obtained from stability limit of Al_2O_3):

$$\mu_O^{min} = \frac{E_{Al_2O_3} - 2E_{Al}}{3}$$

to oxidizing conditions, where μ_O^{max} is defined as the oxygen chemical potential in the gas phase at standard pressure and sintering temperature (2023 K).

The Madelung correction $E_i^{(c)}$ is evaluated using the method proposed in [7, 8] and applied in [9]. The obtained correction can be approximated by the general expression $E_i^{(c)} \approx \alpha q^2$, where α = 0.13 eV.

Electronic band-structure calculations were performed using the Quantum ESPRESSO package [10] with the hybrid PBE0 exchange–correlation functional. Our calculations with a modified PBE0 with a mixing parameter of 0.32 yield $E_g^{PBE0(m)} = 7.7eV$, and relative magnitudes of the band-edge shift follow the proportion $\Delta E_{VBM}/\Delta E_{CBM} \approx 0.65/0.35$. The SIESTA PBE band-structure corrected accordingly by applying the rigid shifts of -2.1eV to the VBM and +1.15 to the CBM, yielding the corrected band gap $E_g = 7.7eV$.

Concentration of defects is given by the equation:

$$c_i = \frac{N_i}{V}\exp\left(-\frac{E_i}{k_B T}\right),$$

where N_i is the number of ways to place a defect of *i* specie in the unit cell,
V is the volume of the YAG unit cell,
T=2023K, which corresponds to the sintering temperature of YAG ceramics.

For defects that contains Si (or Mg) atoms the equation includes the Lagrange multiplier λ_{Si} and the number of Si atoms contained in *i* defect specie k_i^{Si} :

$$c_i = \frac{N_i}{V}\exp\left(-\frac{E_i - \lambda_{Si} k_i^{Si}}{k_B T}\right),$$

Results and Discussion

Our calculations show that Si is incorporated into YAG predominantly on tetrahedral Al sites, forming $Si^{\bullet}_{Al(t)}$ donor defects (Fig. 1(a)), whose charge is compensated mainly by yttrium vacancies. The concentration of isolated cation vacancies depends nonmonotonically on the total Si concentration, reaching a maximum at about 0.05 at.% (relative to the total number of atoms in YAG) and decreasing at higher Si contents due to the formation of Si-vacancy complexes (Fig. 1(b)). This maximum value exceeds that in undoped YAG by about five orders of magnitude. The increase in the yttrium vacancy concentration is expected to accelerate Y diffusion and hence densification during sintering.

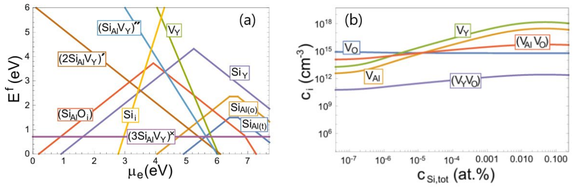

Figure 1. Formation energies of Si-related point defects (a) and concentrations of isolated vacancies and complexes of vacancies as function of dopant concentration (b) in Si doped YAG under intermediate conditions (oxygen partial pressure 10^{-3} Pa, T=2023 K).

Mg is incorporated predominantly on octahedral Al sites as $Mg'_{Al(o)}$ acceptors, which are compensated mainly by doubly positively charged oxygen vacancies. Consequently, Mg doping reduces the cation vacancy concentration and increases the oxygen vacancy concentration. At high Mg contents, the oxygen vacancies are increasingly bound in complexes consisting of one $Mg'_{Al(o)}$ defect and one oxygen vacancy. Since each such complex carries a single positive charge, it compensates an additional $Mg'_{Al(o)}$ defect without creating a new isolated oxygen vacancy, and the concentration of isolated oxygen vacancies saturates.

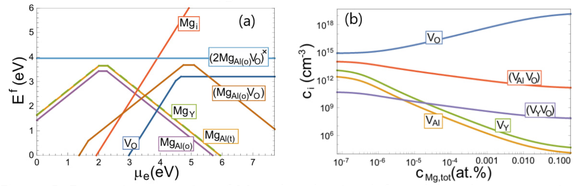

Figure 2. Formation energies of Mg-related point defects (a) and concentrations of isolated vacancies and complexes of vacancies as function of dopant concentration (b) in Mg doped YAG under intermediate conditions (oxygen partial pressure 10^{-3} Pa, T=2023 K).

Results and Discussion

In Si-doped YAG, Mg is incorporated on Al and Y sites as acceptors compensated mainly by $Si^{\bullet}_{Al}$ donors. As the Mg content approaches the Si content, the concentration of isolated cation vacancies decreases by up to twelve orders of magnitude, whereas the oxygen vacancy concentration remains as low as in Si-doped YAG and increases only when Mg is in excess (Fig.3). It is found that Si enhances the solubility of Mg, and therefore more Mg may be available for grain-boundary segregation, which would strengthen the solute drag that is expected to be responsible for the suppression of abnormal grain growth by MgO [11].

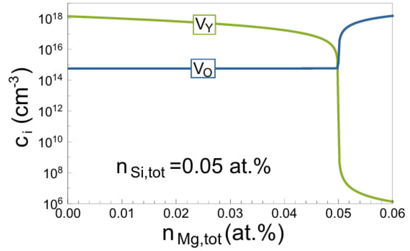

Figure 3. Concentrations of isolated yttrium and oxygen vacancies in YAG co-doped with Si and Mg at a constant Si concentration and varying Mg concentration during sintering under intermediate conditions

Conclusions

1. It is shown that Si doping leads to a significant increase in the equilibrium concentration of cation vacancies and a decrease in the concentration of oxygen vacancies. Mg doping, in contrast, suppresses the formation of cation vacancies and favors the formation of oxygen vacancies.

2. It is found that the concentration of isolated cation vacancies depends nonmonotonically on the Si concentration: it reaches a maximum at relatively low Si content and then decreases with further doping because of the binding of cation vacancies in stable Si-vacancy complexes.

3. Under Si-Mg co-doping, donor and acceptor defects compensate each other, and the concentrations of both cation and oxygen vacancies reach pronounced minima at comparable Si and Mg contents. The resulting low vacancy concentrations are expected to slow down diffusion and hence pore elimination during sintering, which accounts for the high residual porosity reported in [1] for equal Si and Mg concentrations.

References

1. I.O. Vorona, R.P. Yavetskiy, S.V. Parkhomenko, A.G. Doroshenko, O.S. Kryzhanovska, N.A. Safronova, A.D. Timoshenko, A.E. Balabanov, A.V. Tolmachev, V.N. Baumer, J. Eur. Ceram. Soc. 42, 6104 (2022). https://doi.org/10.1016/j.jeurceramsoc.2022.05.017
2. J. M. Soler, E. Artacho, J. D. Gale, A. García, J. Junquera, P. Ordejón, and D. Sánchez-Portal, J. Phys.: Condens. Matter. 14, 2745 (2002). https://doi.org/10.1088/0953-8984/14/11/302
3. M. J. van Setten, M. Giantomassi, E. Bousquet, M. J. Verstraete, D. R. Hamann, X. Gonze, and G.-M. Rignanese, Computer Physics Communications 226, 39 (2018). https://doi.org/10.1016/j.cpc.2018.01.012
4. S. B. Zhang, and J. E. Northrup, Phys. Rev. Lett. 67, 2339 (1991). https://doi.org/10.1103/PhysRevLett.67.2339
5. C. Freysoldt, B. Grabowski, T. Hickel, J. Neugebauer, G. Kresse, A. Janotti, and C. G. Van de Walle, Rev. Mod. Phys. 86, 253 (2014). https://doi.org/10.1103/RevModPhys.86.253
6. J. E. Saal, S. Kirklin, M. Aykol, B. Meredig, and C. Wolverton, JOM 65, 1501-1509 (2013). https://doi.org/10.1007/s11837-013-0755-4
7. N. D. M. Hine, K. Frensch, W. M. C. Foulkes, and M. W. Finnis, Phys. Rev. B 79, 024112 (2009), https://doi.org/10.1103/PhysRevB.79.024112
8. N. D. M. Hine, P. D. Haynes, A. A. Mostofi, and M. C. Payne, J. Chem. Phys. 133, 114111 (2010), https://doi.org/10.1063/1.3492379
9. L. Yu. Kravchenko and D. V. Fil, Phys. Rev. Research 2, 023135 (2020), https://doi.org/10.1103/PhysRevResearch.2.023135
10. P. Giannozzi et al., J. Phys.: Condens. Matter 21, 395502 (2009), https://doi.org/10.1088/0953-8984/21/39/395502
11. T. Zhou, L. Zhang, S. Wei, L. Wang, H. Yang, Z. Fu, Q. Zhang, H. Chen, F. A. Selim, Q. Zhang, J. Eur. Ceram. Soc. 38, 687 (2018). https://doi.org/10.1016/j.jeurceramsoc.2017.09.017